Front. Mater. Sci. 2015, 9(4): 366–372
DOI 10.1007/s11706-015-0308-6

RESEARCH ARTICLE

Preparation and enhancement of ionic conductivity in Al-added garnet-like $Li_{6.8}La_3Zr_{1.8}Bi_{0.2}O_{12}$ lithium ionic electrolyte

Yu XIA, Liang MA, Hui LU, Xian-Ping WANG (✉), Yun-Xia GAO, Wang LIU, Zong ZHUANG, Li-Jun GUO, and Qian-Feng FANG

Key Laboratory of Materials Physics, Institute of Solid State Physics, Chinese Academy of Sciences, Hefei 230031, China

ABSTRACT: Garnet-like $Li_{6.8}La_3Zr_{1.8}Bi_{0.2}O_{12}$ (LLZBO) + *x* mol.% Al_2O_3 (*x* = 0, 1.25, 2.50) lithium ionic electrolytes were prepared by conventional solid state reaction method under two different sintering temperatures of 1000°C and 1100°C. XPS, induced coupled plasma optical emission spectrometer (ICP-OES), XRD and AC impedance spectroscopy were applied to investigate the bismuth valance, lithium concentration, phase structure and lithium ionic conductivity, respectively. Electrical measurement demonstrated that ionic conductivity of Al-added LLZBO compounds could be obviously improved when the sample sintering temperature increased from 1000°C to 1100°C. The highest ionic conductivity 6.3×10^{-5} S/cm was obtained in the LLZBO–1.25%Al sample sintered at 1100°C, in consistent with the lowest activation energy 0.45 eV for the lithium ion migration. The mechanism related with good ionic conductivity in the Al-added LLZBO sample was attributed to the lattice distortion induced by the partial Al substitution at Zr sites, which is helpful to improve the migration ability of Li ions in lattice.

KEYWORDS: garnet lithium electrolyte; cubic $Li_7La_3Zr_2O_{12}$; AC impedance; ionic conductivity; activation energy

Contents

Received May 8, 2015; accepted July 20, 2015

E-mail: xpwang@issp.ac.cn

1 Introduction

With the development of electrochemical power sources, rechargeable all-solid-state lithium batteries (SSLBs) have been considered as one of the most promising next-generation batteries. In contrast with liquid and polymer based lithium ion batteries that may induce serious safety problems, including inflammation, explosion incident and short cycle-life, etc. [1–3], SSLBs generally possess some remarkable advantages, including battery miniaturization, high energy density and high safety. As a key component in

SSLBs, a large number of inorganic oxide and non-oxide electrolytes with amorphous and crystalline structures [4], including NASICON-type phosphates, perovskite-type $La_{(2/3)-x}Li_{3x}TiO_3$ (LLT), Li–β-alumina, Li_3N and Li_4SiO_4, have been investigated till now, but none of them was completely suitable for solid-state electrolytes due to either low lithium ionic conductivity or poor chemical stability. A novel garnet-type material, $Li_7La_3Zr_2O_{12}$ (LLZO) [5] by substituting M with Zr in $Li_5La_3M_2O_{12}$ (M = Ta, Nb) [6], had been reported as a promising candidate used in SSLBs in recent several years because of its high ionic conductivity, good chemical stability with lithium metal as well as wide electrochemical window [5].

However, $Li_7La_3Zr_2O_{12}$ normally crystallizes in tetragonal garnet-type phase with space group $I4_1/acd$ (no.142) [7], which exhibits a poor conductivity of $10^{-6}\,S\cdot cm^{-1}$ at room temperature and therefore greatly limits its actual application as solid lithium electrolytes. Since researchers found that cubic garnet-like $Li_7La_3Zr_2O_{12}$ (space group $Ia\text{-}3d$) with good conductivity (10^{-5}–$10^{-4}\,S\cdot cm^{-1}$) could form if Al_2O_3 was added in the raw materials as a sintering aid [8], numerous experiments had been carried out to understand the role of Al in the formation of cubic phase [9–11], but the underlying mechanism was still controversial. Rangasamy et al. reported that at least 0.204 mol Al was required to stabilize the cubic phase in 1 mol $Li_7La_3Zr_2O_{12}$ by substituting Li [8]. This opinion was further supported by Ahn et al. [12], and in their investigation the incorporation of Al into the $Li_7La_3Zr_2O_{12}$ lattice was found to not only effectively stabilize the cubic garnet phase to room temperature but also greatly increase the concentration of Li-ion vacancies, which was suggested as the main reason for the enhancement of Li-ion conductivity, from $1.1\times10^{-6}\,S\cdot cm^{-1}$ for tetragonal phase to $8.5\times10^{-5}\,S\cdot cm^{-1}$ for cubic phase. As for the accommodation of Al in $Li_7La_3Zr_2O_{12}$ lattices, Kuhn et al. [13] believed that in the condition of relatively low Al concentration, the dopant Al^{3+} ions mainly occupied at Li^+ sites. In terms of electrically neutral compensation principle, the extra lithium vacancies would be thus formed. But with gradually increasing Al concentration, La^{3+}/Zr^{4+} ions in $Li_7La_3Zr_2O_{12}$ lattices would be progressively replaced by Al^{3+} ions. A latest investigation [14] even revealed that besides the effective occupation of Al^{3+} ions at Zr^{4+} sites, partial Al substitution could facilitate the transition to cubic modification.

Considering from electrical properties, partial substitution of tetravalent cations by trivalent Al^{3+} in solid electrolytes had been reported to effectively enhance its electrical conductivity. As an example for $La_{(2/3)-x}Li_{3x}TiO_3$ electrolyte [15], its ionic conductivity at 23 K could be obviously improved from 1.08×10^{-3} to 1.59×10^{-3} $S\cdot cm^{-1}$ after partial substitution of Ti^{4+} by Al^{3+}, and the reason was interpreted as substitution-induced bond-strength change. So far, the effect and mechanism of Al ions on ionic accommodation and conductivity are rarely concerned in stabilized cubic $Li_7La_3Zr_2O_{12}$ although a series of researches have been carried out to investigate the influence of Al stabilization on tetragonal $Li_7La_3Zr_2O_{12}$ electrolyte. In this paper, different amounts of γ-Al_2O_3 were added into Bi-stabilized cubic $Li_7La_3Zr_2O_{12}$ compounds fabricated at different sintering temperatures of 1000°C and 1100°C, and the effects of partial Al substitution on structure, lithium concentration and ionic conductivity in Bi-stabilized cubic $Li_{6.8}La_3Zr_{1.8}Bi_{0.2}O_{12}$ (LLZBO) were investigated through X-ray diffraction (XRD), induced coupled plasma optical emission spectrometer (ICP-OES) and alternate current (AC) impedance spectroscopy, respectively.

2 Experimental

High pure commercial reagents Li_2CO_3 (99.9%), La_2O_3 (99.9%), ZrO_2 (99.9%), γ-Al_2O_3 (99.9%) and Bi_2O_3 (99.9%) were obtained from Aladdin In. Co. and J&K Scientific Ltd., in which γ-Al_2O_3 was used as a source of Al doping. All samples in our investigation were prepared via conventional solid-state reaction method. Prior to sample preparation, the raw material La_2O_3 was pre-heated at 900°C for 12 h to remove residual carbon dioxide and moisture. Besides extra 10 wt.% Li_2CO_3 to compensate the Li loss induced by high-temperature sintering, La_2O_3, ZrO_2, γ-Al_2O_3 and Bi_2O_3 were precisely weighed according to the stoichiometry of targeted composition. During the sample preparation, Bi-doped $Li_7La_3Zr_2O_{12}$ compounds with chemical formula of $Li_{7-x}La_3Zr_{2-x}Bi_xO_{12}$ (LLZBO, $x = 0.2-0.6$) were firstly synthesized in order to check whether the Bi doping could effectively stabilize the cubic $Li_7La_3Zr_2O_{12}$ phase to room temperature. And then, series $Li_{6.8}La_3Zr_{1.8}Bi_{0.2}O_{12}$ + x mol.% γ-Al_2O_3 (x = 0, 1.25, 2.5) electrolytes were further prepared to investigate the effect of extra aluminum addition on the ionic conductivity of cubic LLZBO samples. To obtain pure phase, all of the raw materials were mixed initially by planetary ball-milling in anhydrous ethanol with agate balls. Then, the mixed powders were sintered at 950°C for

6 h. After being carefully ground, the calcined powders were pressed into molds to form cylindrical wafers with a pressure of 400 MPa, and the second sintering temperatures and times were determined as 1000°C and 1100°C for 9 h, respectively.

X-ray photoemission spectra (XPS) were recorded on a VG ESCALAB 250 spectrometer using Al Kα radiation with an energy step size of 0.05 eV to exam Bi 4*f* photoemission spectra of the LLZBO compounds. Cu Kα radiation (X'pert MPD PRO diffractometer) was used to determine the crystal structures and lattice parameters of the investigated samples at room temperature and the 2θ range covered from 10° to 70° with a step size of 0.033°. Rietveld program based on a pseudo-Voigt function was performed to refine the whole XRD patterns. The concentration of lithium was determined by ICP-OES (Optima 7300 DV).

Both sides of LLZBO samples used in the ionic conductivity measurement were painted by silver electrodes, which were formed by drying Ag paste (Uninwell Inc.) at 150°C for 45 min. The impedance spectra were isothermally measured in air with an impedance analyzer (Hioki 3531 Z-Hitester frequency response analyzer) in the frequency range of 42 Hz to 5 MHz under amplitude of 0.5 V. Zview software was used to fit the impedance spectra and determine the impedance of the samples. The lithium ionic conductivity was calculated using the following equation: $\sigma = (1/R)(d/A)$, where σ is the ionic conductivity, R is the impedance, d is the pellet thickness, and A is the pellet area. The average size of the sample pellets was 11–13 mm in diameter and 2–2.3 mm in thickness.

3 Results and discussion

3.1 Phase of $Li_{7-x}La_3Zr_{2-x}Bi_xO_{12}$ compounds

Figure 1 presents the Bi 4*f* photoemission spectrum of LLZBO sample, and two main peaks are observed, which locate at 164.2 and 158.7 eV, respectively. The peak shape and peak position are very close to the Bi 4*f* feature in $NaBiO_3$ with Bi in the typical V valance state [16], evidencing that the Bi element in the $Li_7La_3Zr_2O_{12}$-based compound only exhibits single V valence and no other valance state appears.

To further understand the phase structure of Bi-stabilized $Li_7La_3Zr_2O_{12}$ compounds, Fig. 2(a) gives Rietveld refinement results of the XRD pattern of a $Li_{7-x}La_3Zr_{2-x}Bi_xO_{12}$ sample with $x = 0.3$, and corresponding powder sample

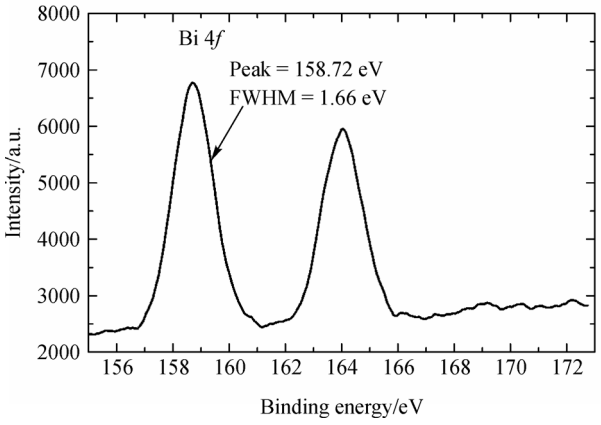

Fig. 1 XPS of Bi 4*f* for a $Li_{7-x}La_3Zr_{2-x}Bi_xO_{12}$ compound.

was ground from the ceramic pellet sintered at 1000°C for 6 h. As noted that all of the observed diffraction peaks in the XRD pattern can be well indexed as a cubic garnet-like structure (space group: *Ia*-3*d*, which evidences that the Bi substitution at Zr sites can effectively stabilize the cubic phase to room temperature. For other LLZBO compounds with different Bi concentration, similar Rietveld fitting results can be also obtained. Figure 2(b) shows the evolution of the lattice parameter of $Li_{7-x}La_3Zr_{2-x}Bi_xO_{12}$ samples with the Bi concentration, where the cell parameter is found to increase linearly with increasing the Bi content x in terms of the Vegard's law. The reason for the increase of cell parameter is ascribed to the larger ionic radius of Bi^{5+} (0.90 nm) in comparison with that of Zr^{4+} (0.86 nm) under the same six-coordinate environments. From another side, the regular variation of cell parameter induced by Bi addition provides a key proof for the effective substitution of Zr^{4+} ions by Bi^{5+} ions in the garnet lattice.

3.2 Phase of $Li_{6.8}La_3Zr_{1.8}Bi_{0.2}O_{12} + x$ mol.% γ-Al_2O_3

Figure 3 presents XRD patterns of the γ-Al_2O_3-added $Li_{6.8}La_3Zr_{1.8}Bi_{0.2}O_{12}$ samples sintered at 950°C for 6 h. The corresponding γ-Al_2O_3 contents are 0, 1.25 and 2.5 mol.%, respectively. To describe simply thereafter, the samples are in turn labeled as LLZBO for $Li_{6.8}La_3Zr_{1.8}Bi_{0.2}O_{12}$, LLZBO–1.25%Al for $Li_{6.8}La_3Zr_{1.8}Bi_{0.2}O_{12}$ + 1.25 mol.% Al_2O_3 and LLZBO–2.5%Al for $Li_{6.8}La_3Zr_{1.8}Bi_{0.2}O_{12}$ + 2.5 mol.% Al_2O_3 in terms of their nominal stoichiometry. As can be seen from Fig. 3, all of the investigated samples exhibit a typical garnet-type structure with cubic symmetry, and no other impurity phases are found in the XRD patterns. The cell parameter of the γ-

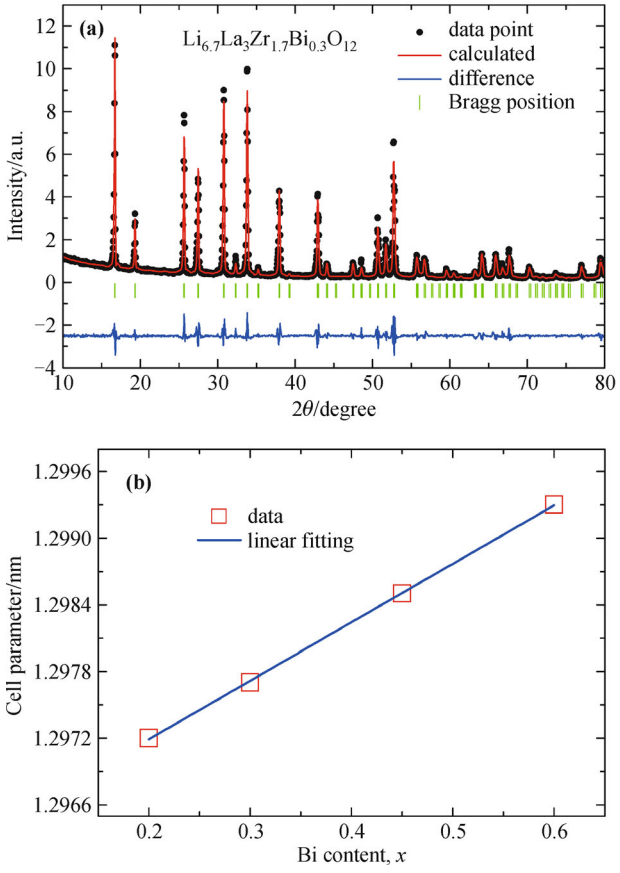

Fig. 2 **(a)** Results of XRD Rietveld refinement for the Bi-stabilized cubic $Li_{6.7}La_3Zr_{1.7}Bi_{0.3}O_{12}$ sample using a space group *Ia*-3*d*. **(b)** Variation of the cell parameter of Bi-stabilized $Li_{7-x}La_3Zr_{2-x}Bi_xO_{12}$ samples as a function of the Bi content.

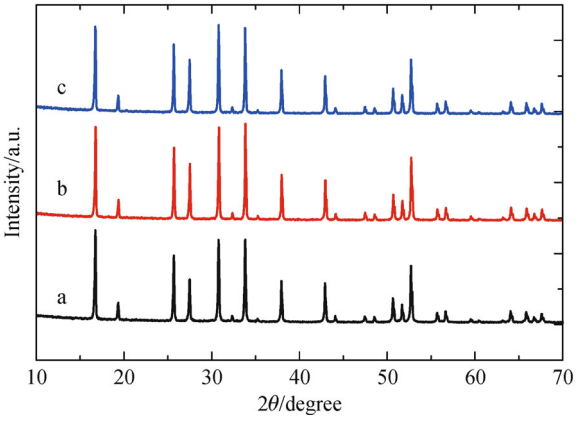

Fig. 3 Powder XRD patterns of LLZBO and Al-added LLZBO samples sintered at 950°C for 6 h: LLZBO (a); LLZBO–1.25%Al (b); LLZBO–2.5%Al (c).

Al_2O_3-added LLZBO samples deduced by the Rietveld refinement is about 12.99(7) Å, which is very close to the previously reported value of 13.0035 Å [17]. As for the Li concentration in the LLZBO compound sintered at 950°C, the ICP analysis reveals that the Li concentration in the LLZBO–2.5%Al is about 4.98 wt.%, as shown in Table 1, which is higher than the value of 4.61 wt.% for LLZBO and 4.52 wt.% for LLZBO–1.25%Al, respectively. This result implies that suitable aluminum addition can weaken the tendency of lithium evaporation in LLZBO compounds, in well consistent with the reported results in Ref. [14].

Table 1 Li concentration in LLZBO and Al-added LLZBO samples sintered at 950°C determined by ICP analysis

Sample	Li content /wt.%
LLZBO	4.61
LLZBO–1.25%Al	4.52
LLZBO–2.5%Al	4.98

3.3 Ionic transport properties

To investigate the influence of temperature on ionic conductivity in the γ-Al_2O_3-added LLZBO compounds, two higher sintering temperatures (1000°C and 1100°C) are chosen after the initial sintering at 950°C for 6 h. Figures 4(a) and 4(b) give the typical room-temperature (RT) impedance spectra of different Al-added LLZBO pellets sintered at 1000°C and 1100°C for 9 h, respectively. As can be seen from this figure, the Nyquist plots for all the investigated samples are composed of one pressed semicircle and a tail. According to the Boukamp model [18], the impedance plots for ionic migration in solid electrolytes can be described by series R_iQ_i (i = 1, 2, 3) equivalent circuits in general, where R_i and Q_i represent resistances and universal capacitances of the bulk (i = 1), grain boundary (i = 2) and electrodes (i = 3), respectively. In this investigation, only one pressed semicircle is observed at the higher frequency side, the reason of which is mainly owing to the overlap of the bulk and grain boundary response. The tail at the low-frequency side is caused by an almost solely capacitive behavior of material/Ag electrodes, which indicates their ionic blocking nature under the given measurement conditions. Owing to the overlap of grain and grain boundary semicircles that results in the difficulty of gain and grain boundary resistance separation, the total resistance is thus used to describe the ionic conduction properties of LLZBO-based samples.

In terms of nonlinear fitting based on the R_iQ_i model, the total resistance (R) is determined, and the corresponding fitting profiles using Zview software are shown in Figs. 4(a) and 4(b). The total ionic conductivity at room temperature for all the investigated samples is listed in Table 2. As can be seen, the Li-ion conductivity of LLZBO-based pellets sintered at 1000°C is relatively poor,

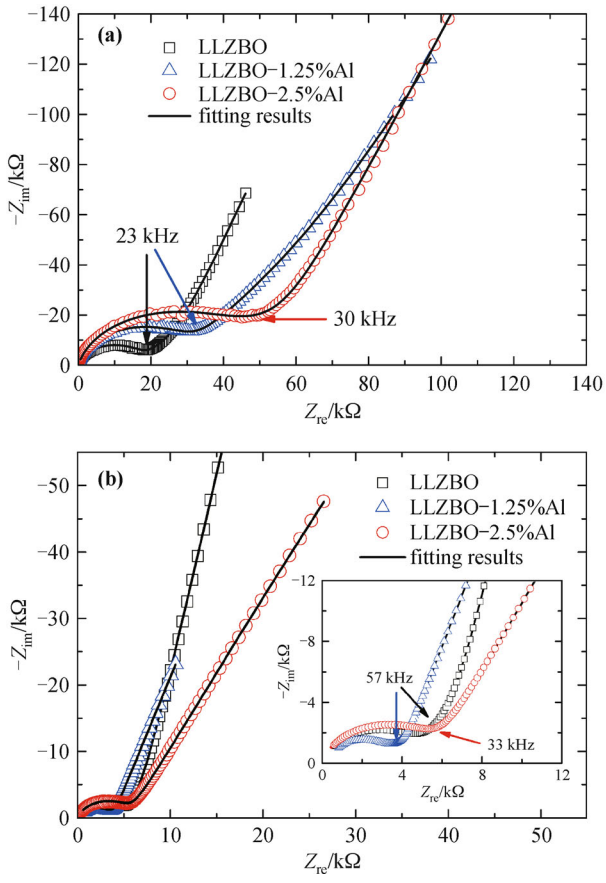

Fig. 4 Impedance plots of LLZBO and Al-added LLZBO pellets measured in air at room temperature: **(a)** sintered at 1000°C for 9 h; **(b)** sintered at 1100°C for 9 h. Insert: Local enlarged high-frequency region of the same impedance spectra.

and the conductivity decreases gradually from 8.1×10^{-6} S·cm^{-1} for the LLZBO sample to 3.6×10^{-6} S·cm^{-1} for the LLZBO–2.5%Al sample with increasing Al amount. In contrast to that of the samples sintered at 1000°C, the Li-ion conductivity of the LLZBO-based pellets sintered at 1100°C is found to be obviously enhanced, and the highest conductivity of 6.3×10^{-5} S·cm^{-1} is observed in the LLZBO–1.25%Al sample. In the same sintering condition, the ionic conductivity of LLZBO is only 2.6×10^{-5} S·cm^{-1} due to the lack of Al doping, which exhibits the poorest conductivity among all the investigated pellets sintered at 1100°C. This result indicates that at higher sintering temperature, the Al addition can effectively improve the ionic conductivity of LLZBO compounds.

Figures 5(a) and 5(b) present the Li-ion conductivity as a function of $1/T$ for the sintered samples at two different temperatures of 1000°C and 1100°C, respectively. It is found that in the whole investigated temperature range 30°C–110°C, the conductivity is closely related with sintering temperature and Al concentration. For the case of 1000°C sintering, the Al-free LLZBO sample exhibits better ionic conductivity in comparison with the Al-added LLZBO samples. On the contrary, the conductivity of the Al-added LLZBO samples is higher than that of Al free LLZBO sample once the sintering temperature is further enhanced up to 1100°C, and the best conduction property is observed in the 1.25% Al-added LLZBO sample in the whole investigation temperature range.

To further understand the migration properties of lithium ions in the LLZBO-based compounds, the activation energy of lithium ions is determined in term of the following Arrhenius relation: $\sigma T = A\exp[-E_a/(kT)]$, where A is the pre-exponential factor, T is the absolute temperature, E_a is the activation energy, and k is the Boltzmann's constant. In Figs. 5(a) and 5(b), the corresponding linear fitting results are given in detail, and activation energy parameters for lithium ion diffusion are thus determined from the slope of the fitting lines, as summarized in Table 2. As can be seen, the value of 0.45 eV for the LLZBO–1.25%Al sample sintered at 1100°C is the lowest among all the investigated samples, which is consistent with its best ionic conductivity.

As revealed by the experimental results above, the conductivity of LLZBO compounds is closely related with the Al concentration and the sintering temperature, and the best Li conductivity appears in the LLZBO–1.25%Al sample sintered at 1100°C. It is worthy noting that for the Bi-stabilized LLZO compound, it is actually cubic modification. Therefore the Al addition is not aimed to stabilize the cubic garnet phase. The difference of ionic conductivity among the investigated samples should be ascribed to the different concentration of Li ions as well as the change of Li ion migration channels in lattices induced by the Al addition. It was reported that in the Al-added

Table 2 RT conductivity and Li migration activation energy for LLZBO and Al-added LLZBO samples sintered at 1000°C and 1100°C, respectively

Sample	RT conductivity /(S·cm^{-1})		Activation energy /eV	
	1000°C/9 h	1100°C/9 h	1000°C/9 h	1100°C/9 h
LLZBO	8.1×10^{-6}	2.6×10^{-5}	0.51	0.51
LLZBO–1.25%Al	5.04×10^{-6}	6.31×10^{-5}	0.54	0.45
LLZBO–2.5%Al	3.6×10^{-6}	4.3×10^{-5}	0.55	0.49

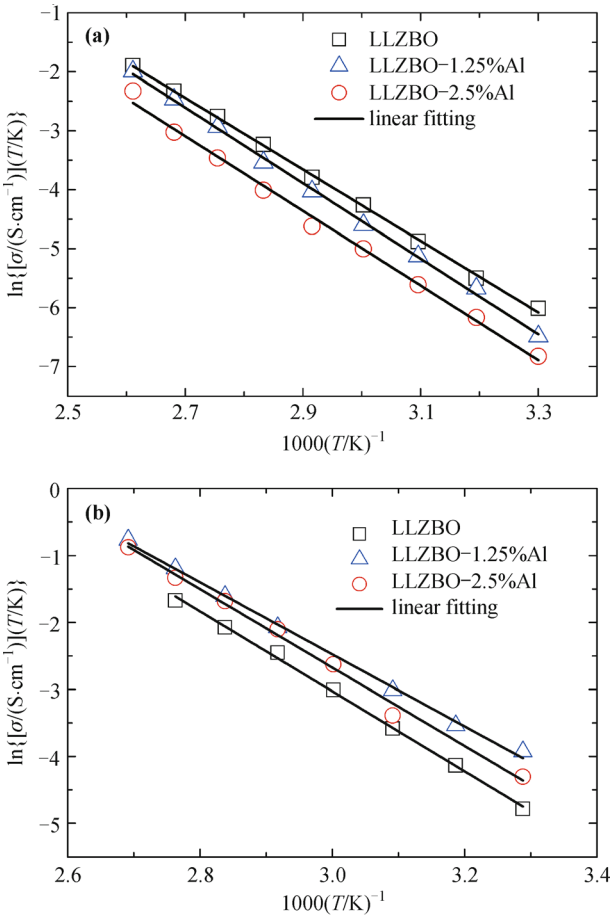

Fig. 5 Arrhenius plots of LLZBO and Al-added LLZBO pellets measured in the temperature range from 30°C to 110°C: **(a)** sintered at 1000°C for 9 h; **(b)** sintered at 1100°C for 9 h.

LLZO-based electrolytes, Al^{3+} ions can not only occupy the Li positions in the garnet-like lattices, but also reside on a tetrahedral site near Zr and Al vacancy once the sintering temperature reached up to or more than 1100°C [14]. According to this consideration, the improvement of ionic conductivity in the Al-added LLZBO samples can be suggested to originate from the partial Al substitution at the Zr site, which will distort the LLZBO lattices and is therefore helpful to improve the migration ability of Li ions.

4 Conclusions

Series of $Li_{6.8}La_3Zr_{1.8}Bi_{0.2}O_{12}$ + x mol.% Al_2O_3 (x = 0, 1.25, 2.50) compounds with cubic garnet structure were synthesized through traditional solid state reaction method. In order to understand the influence of sintering temperature on Li conductivity, two different temperatures of 1000°C and 1100°C were chosen to sinter LLZBO-based pellets with or without Al_2O_3. In the case of sintering at 1000°C, the Al_2O_3-added LLZBO compounds exhibit poor ionic conductivity, in which RT conductivity decreases gradually from $8.1\times10^{-6}\,S\cdot cm^{-1}$ for the Al-free LLZBO sample to $3.6\times10^{-6}\,S\cdot cm^{-1}$ for the LLZBO–2.5%Al sample with increasing the Al amount. It is interesting to note that once the sintering temperature reaches up to 1100°C, the conduction property of LLZBO-based compounds will be greatly improved, and the highest conductivity $6.3\times10^{-5}\,S\cdot cm^{-1}$ is observed in the 1.25% Al-added LLZBO sample, which is consistent with its lowest activation energy, 0.45 eV, for lithium ion migration. The possible mechanism related with the enhancement of conductivity is suggested to originate from the lattice distortion induced by partial Zr substitution with Al at a higher sintering temperature of 1100°C. Such lattice distortion is helpful to improve the diffusion ability of Li ions in lattice, as evidenced by results of migration activation energy of lithium ions.

Acknowledgements This work was financially supported by the National Natural Science Foundation of China (Grant Nos. 11374299, 11405203 and 51401203).

References

[1] Thangadurai V, Narayanan S, Pinzaru D. Garnet-type solid-state fast Li ion conductors for Li batteries: critical review. Chemical Society Reviews, 2014, 43(13): 4714–4727

[2] Zhu J, Xu Z, Lu B G. Ultrafine nanoparticles decorated $NiCo_2O_4$ nanotubes as anode material for high-performance supercapacitor and lithium-ion battery applications. Nano Energy, 2014, 7: 114–123

[3] Zhu J, Chen L B, Xu Z, et al. Electrospinning preparation of ultralong aligned nanofibers thin films for high performance fully flexible lithium-ion batteries. Nano Energy, 2015, 12: 339–346

[4] Thangadurai V, Weppner W. Effect of sintering on the ionic conductivity of garnet-related structure $Li_5La_3Nb_2O_{12}$ and In- and K-doped $Li_5La_3Nb_2O_{12}$. Journal of Solid State Chemistry, 2006, 179(4): 974–984

[5] Murugan R, Thangadurai V, Weppner W. Fast lithium ion conduction in garnet-type $Li_7La_3Zr_2O_{12}$. Angewandte Chemie International Edition, 2007, 46(41): 7778–7781

[6] Thangadurai V, Kaack H, Weppner W. Novel fast lithium ion conduction in garnet-type $Li_5La_3M_2O_{12}$ (M = Nb, Ta). Journal of the American Ceramic Society, 2003, 86(3): 437–440

[7] Awaka J, Kijima N, Hayakawa H, et al. Synthesis and structure analysis of tetragonal $Li_7La_3Zr_2O_{12}$ with the garnet-related type structure. Journal of Solid State Chemistry, 2009, 182(8): 2046–

2052

[8] Rangasamy E, Wolfenstine J, Sakamoto J. The role of Al and Li concentration on the formation of cubic garnet solid electrolyte of nominal composition $Li_7La_3Zr_2O_{12}$. Solid State Ionics, 2012, 206: 28–32

[9] Hubaud A A, Schroeder D J, Key B, et al. Low temperature stabilization of cubic $(Li_{7-x}Al_{x/3})La_3Zr_2O_{12}$: role of aluminum during formation. Journal of Materials Chemistry A: Materials for Energy and Sustainability, 2013, 1(31): 8813–8818

[10] Wang X P, Xia Y, Hu J, et al. Phase transition and conductivity improvement of tetragonal fast lithium ionic electrolyte $Li_7La_3Zr_2O_{12}$. Solid State Ionics, 2013, 253: 137–142

[11] Lee J M, Kim T, Baek S W, et al. High lithium ion conductivity of $Li_7La_3Zr_2O_{12}$ synthesized by solid state reaction. Solid State Ionics, 2014, 258: 13–17

[12] Ahn J H, Park S Y, Lee J M, et al. Local impedance spectroscopic and microstructural analyses of Al-in-diffused $Li_7La_3Zr_2O_{12}$. Journal of Power Sources, 2014, 254: 287–292

[13] Düvel A, Kuhn A, Robben L, et al. Mechanosynthesis of solid electrolytes: preparation, characterization, and Li ion transport properties of garnet-type Al-doped $Li_7La_3Zr_2O_{12}$ crystallizing with cubic symmetry. Journal of Physical Chemistry C, 2012, 116 (29): 15192–15202

[14] Raskovalov A A, Il'ina E A, Antonov B D. Structure and transport properties of $Li_7La_3Zr_{2-0.75x}Al_xO_{12}$ superionic solid electrolytes. Journal of Power Sources, 2013, 238: 48–52

[15] He L X, Yoo H I. Effect of B-site ion (M) substitution on the ionic conductivity of $(Li_{3x}La_{2/3-x})_{1+y/2}(M_yTi_{1-y})O_3$ (M = Al, Cr). Electrochimica Acta, 2003, 48(10): 1357–1366

[16] Kulkarni G U, Vijayakrishnan V, Rao G R, et al. State of bismuth in $BaBiO_3$ and $BaBi_{1-x}Pb_xO_3$: Bi 4*f* photoemission and Bi L_3 absorption spectroscopic studies. Applied Physics Letters, 1990, 57(17): 1823–1824

[17] Xie H, Alonso J A, Li T, et al. Lithium distribution in aluminum-free cubic $Li_7La_3Zr_2O_{12}$. Chemistry of Materials, 2011, 23(16): 3587–3589

[18] Boukamp B A. Equivalent Circuit, Users Manual. 2nd ed. The Netherlands: University of Twente, 1989, 1